A Pi2-associated dusk-to-dawn currents in the midnight sector as observed at $L = 6.6$ during multiple Pi2 onsets

O. Saka[1], H. Akaki[2], and D. N. Baker[3]

[1]*Department of Physics, Kurume National College of Technology, Kurume 830-8555, Japan*
[2]*Department of Earth and Planetary Science, Kyushu University, Fukuoka 812-8581, Japan*
[3]*Laboratory for Atmospheric and Space Physics, University of Colorado, Boulder, CO 80309, U.S.A.*

We examined the magnetic fields and energetic particle data from geosynchronous satellites GOES 6 and S/C1984-129 during the multiple onset of Pi2. We found that the energetic particle injection in the midnight sector was associated with the consecutive Pi2 onset. The magnetometer on board GOES 6 at the midnight sector detected the increase of the field inclination as well as a decrease of the field magnitudes during the Pi2 events. We suggest that such a field reconfiguration could be provoked by the formation of the dusk-to-dawn currents in the vicinity of the geosynchronous altitudes. The present study supports the Pi2 model that the impulsive dusk-to-dawn current and field-aligned current diverted from it are a source of Pi2 pulsation in the midnight magnetosphere.

Key words: Magnetospheric substorm, Pi2 onset, plasma dynamics, geosynchronous altitudes.

1. Introduction

The onset of magnetospheric substorms is accompanied by many kinds of disturbances in the ionosphere and the magnetosphere (Baker *et al.*, 1996). Auroral break-up, particle injections, and Pi2 magnetic pulsations are some of the observable manifestations at the substorm expansion onset (Akasofu, 1964; Reeves *et al.*, 1990; Yeoman *et al.*, 1994; Saka *et al.*, 1996). Numerous investigations about these manifestations have been carried out for the last few decades (Olson, 1999 and references therein). The Pi2 band oscillations in the magnetosphere have been considered to be composed of a transverse mode of the field-aligned current perturbation (Sakurai and McPherron, 1983; Takahashi *et al.*, 1996; Saka *et al.*, 1996), and poloidal mode in the inner magnetosphere (Takahashi *et al.*, 1995). The poloidal mode has been interpreted as being excited by the initial jump of the H component in the near Earth magnetotail associated with the field dipolarization at the substorm onset (Yumoto *et al.*, 1989). The Pi2 observations in the inner magnetosphere indicate a nodal structure of the poloidal mode oscillations (Takahashi *et al.*, 1992). Recently, a simulation study by Fujita *et al.* (2000, 2002) showed that the eastward (dusk-to-dawn) currents set up impulsively in the midnight sector reasonably reproduce those Pi2 signatures, both toroidal and poloidal modes in the near Earth magnetosphere. Such eastward currents are supposed to be excited during the substorm expansion onset by the breaking of the Earthward fast flow (Shiokawa *et al.*, 1997) and/or by the pressure balance between injected plasmas and magnetic fields of the inner magnetosphere (Saka *et al.*, 1997).

Examination of the particles and field changes at geosyn-

chronous altitudes that occurred during multiple Pi2 onsets is carried out here by use of magnetometer and particle data from the GOES 6 and S/C1984-129 satellites in the midnight sector.

2. Observations

Multiple Pi2 onsets were detected in the post-midnight sector on 12 April 1986 by the ground magnetometer at the dip-equator (Huancayo, Peru, 1.44°N, 355.9° in geomagnetic coordinates, 12.1°S, 75.2°W in geographic coordinates). Meanwhile, the particle detector and the magnetometer on board, respectively, geosynchronous satellite S/C1984-129 and GOES 6 were in the midnight sector.

The ground magnetometer signature showing multiple Pi2 onsets and concurrent particle and magnetic field signatures (as observed at geosynchronous altitudes by S/C1984-129 and GOES 6) is depicted in Fig. 1. The eight Pi2 trains were seen to occur in a 2-hour interval spanning from 0630 UT to 0830 UT as demonstrated in dynamic power spectra in the third panel (c) and wave forms in the forth panel (d) (marked A through H). The vertical bars indicate the onset of Pi2s. The Pi2 onsets, "B", "C", "D", "F", "G", and "H" were accompanied by a clear injection signature in the midnight sector (2036 LT at 0700 UT) for (a) electrons in the energy range 30–140 keV and (b) protons in the range 72–153 keV. For the event "F", the electron event would overlap the previous event "E", while the proton event is evident. The electron injection associated with the Pi2 onset "A" was detected by S/C1982-019 at dawn sector. Consequently, the Pi2 onsets "A" through "H" are associated with particle injections at geosynchronous altitudes. In the fifth panel (e), field magnitudes as observed by GOES 6 (2348 LT at 0700 UT) are plotted. During the course of the event "C" and "D", no magnetometer data were available. It is apparent that the field magnitudes decreased except for the
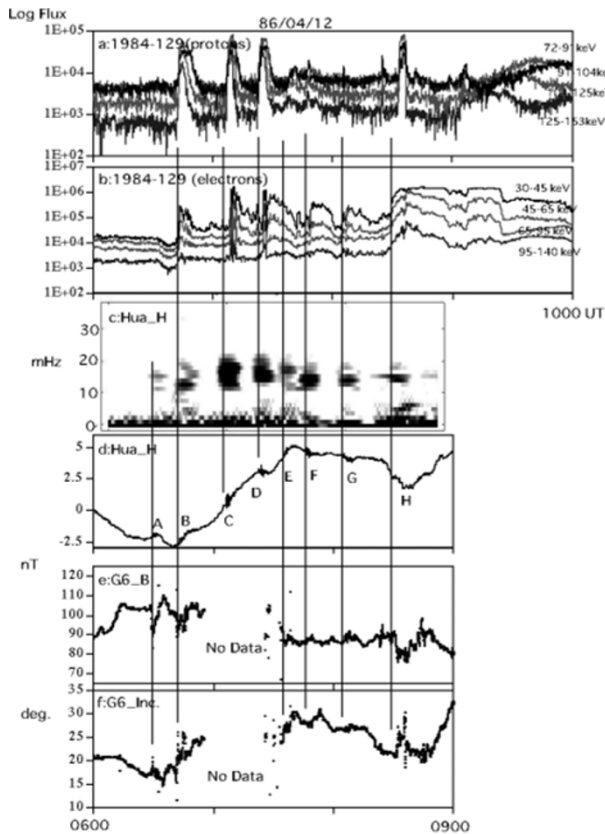
Fig. 1. A multiple Pi2 event for the interval 0600 UT–1000 UT 12 April 1986. (a) The energetic proton and (b) electron flux data (cm^{-2}s^{-1}sr^{-1}) in differential channels of S/C1984-129 in the midnight sector. The energy ranges are 72–91 keV, 91–104 keV, 104–125 keV, 125–153 keV for protons; 30–45 keV, 45–65 keV, 65–95 keV, 95–140 keV for electrons. (c) Power spectra of the H component of the ground magnetometer data (Huancayo, Peru) calculated by FFT method (sampled at 3 sec, 12.8 min interval with 1 min shift). (d) Plot of the H component of the ground data (Huancayo) (in nT, positive northward). (e) Field magnitude B and (f) Field line inclination (measured from the equatorial plane, positive northward) of the GOES 6 magnetometer data at geosynchronous altitudes. The vertical bars indicate an onset of Pi2 labeled "A" through "H".
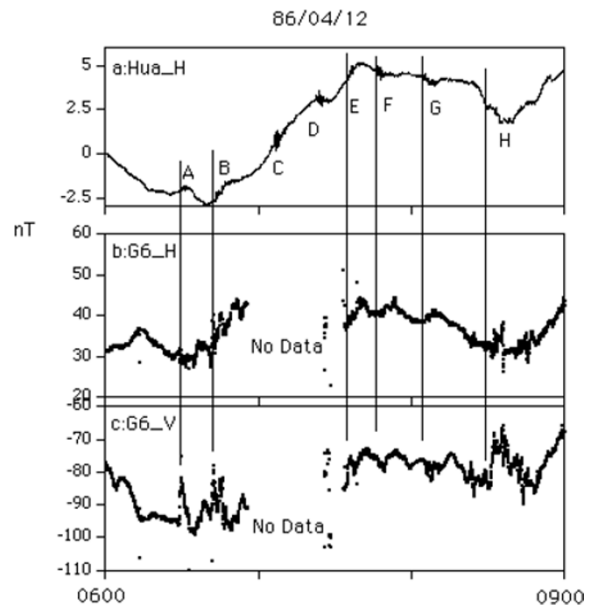

Fig. 2. Same as Fig. 1 but for (a) Plot of the H component of the ground station, Huancayo. (b) H component and (c) V component of GOES 6 magnetometer data. The particle flux and Power spectra of Pi2 are not presented.

event "F" and "G". The decreased level reached to 10–15 nT for the event "A", "B", and "H". It was about 5 nT for the event "E". The decreasing intervals were comparable to the Pi2 interval ranging from 5–10 min. The magnetometer data of GOES 6 are composed of H, V, D components in the dipole coordinate system: H is northward anti-parallel to the dipole axis, V is radial outward, and D is azimuthally eastward. The amplitudes in the H, V and D component are in the ranges of $30 \sim 40$ nT, $-70 \sim -100$ nT, $-5 \sim 30$ nT, respectively for the interval of events. We then supposed that the field magnitudes examined were mostly affected by the V component. Indeed, as demonstrated in the bottom panel of Fig. 2, the V component increased tailward to decrease the field magnitudes for the events "A", "B", "E", and "H", which is anti-parallel to the background field lines. In contrast, the V component change was earthward and was parallel to the background field lines for the event "F" and "G". Consequently, the field magnitudes increased. In the bottom panel (f) of Fig. 1, field line inclinations are plotted. The field line inclination increased (dipolarized) except for the

events "F" and "G". Shrinkage of the field lines by the addition of anti-parallel component (tailward component) to the background field lines could be a primary cause of a dipolarization. When the field line change was nearly parallel to the background field lines (event "F" and "G"), no significant dipolarization occurred. It is apparent that the field magnitudes and the field line inclinations as observed by the GOES 6 magnetometer during the Pi2 event can be understood mostly by the field changes in the V component. We believe that we could attribute the Pi2-associated field line changes to a set-up of the dusk-to-dawn currents at geosynchronous altitudes. In what follows, we simulate the field line changes produced by the dusk-to-dawn currents.

3. A Model of Geomagnetic Field Change by Dusk-to-dawn Current

In this model, the dusk-to-dawn current was assumed to form a sheet current at an L-value between 6 and 8 with a finite thickness of 1 Re. The simulation results are shown in Fig. 3. In this calculation, the Tsyganenko 89 model is employed to describe a background field in (a) (upper left panel). The field vectors produced by the dusk-to-dawn current as described in (b) (upper right panel) are superimposed on the background fields to evaluate the current effect. The results are demonstrated in (c) (middle panel) and (d) (bottom panel) of the figure. As can be seen in the bottom panel, negative B changes are distributed in the green to yellow color area while positive B changes are distributed in the area colored purple to red. The area of light blue is where the changes of the field magnitudes vanish. This area is referred to as a demarcation region. The negative B maximized at the lower-right portion of the current sheet, where the field changes by the dusk-to-dawn current, is mostly anti-parallel to the background field lines. As a result, the field magni-
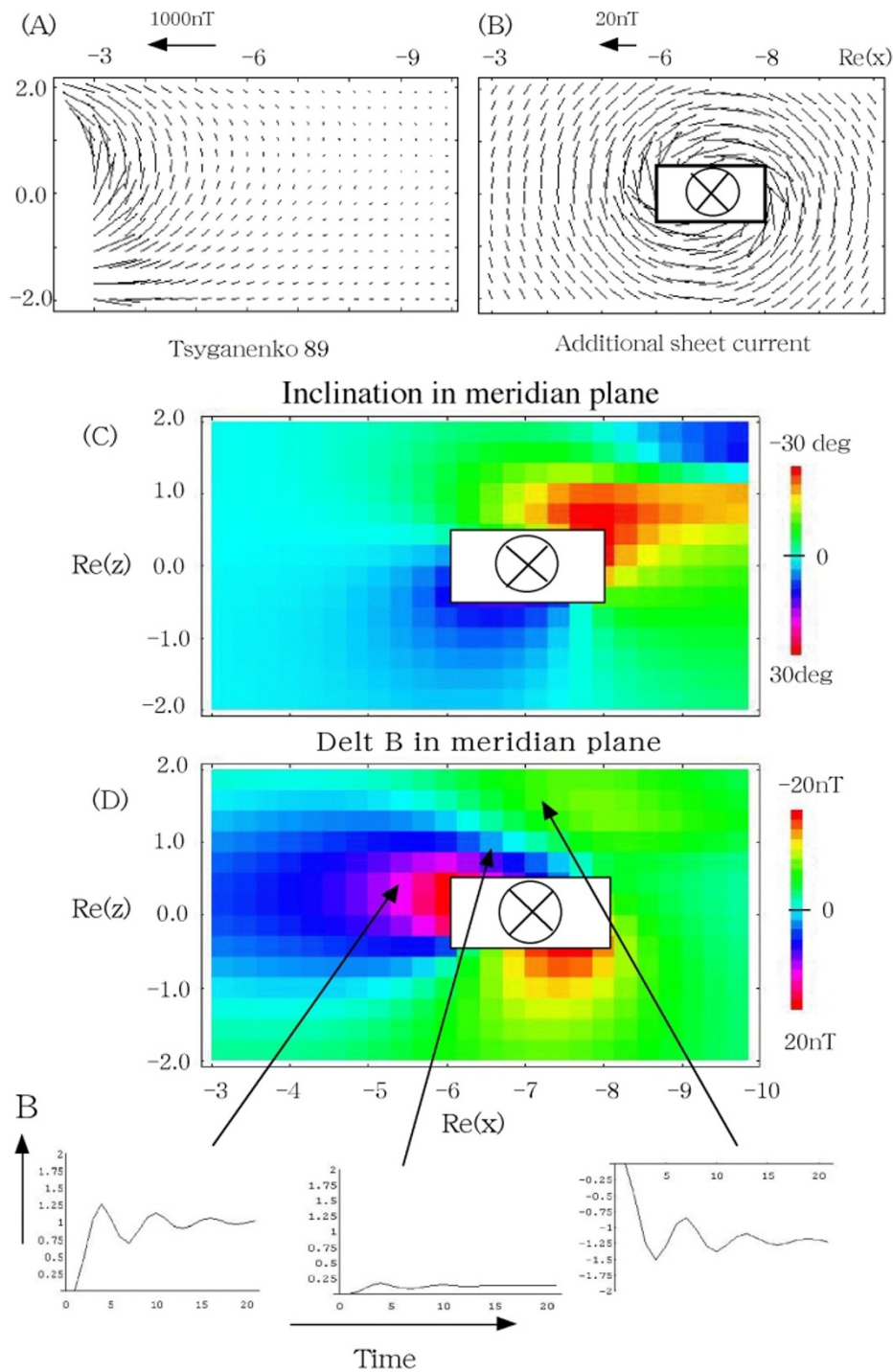
Fig. 3. (a): Background field line vectors in the midnight meridian ($X = 3$–10 Re, $Z = -2$–2 Re) calculated by use of the Tsyganenko 89 model. The scale of the field line vector is shown in the top of the panel. (b): Field line vectors in the midnight meridian produced by the dusk-to-dawn current sheet (shown by the rectangle) located at an L between 6 and 8 in the midnight sector. The scale of the field line vector is shown in the top of the panel. (c): Distribution of field line inclination (see text). (d): Meridional cross section of the changes of the field magnitude B. The current sheet is marked by the rectangle in the panel. Below the bottom panel, a time variation of the field magnitudes caused by the damped modulation of the current intensity is schematically illustrated at three different positions; from left to right, positive B region, demarcation region, and negative B region.

tude increases only in the front portion of the dusk-to-dawn currents, where the current-induced fields have a component parallel to the background field lines. This area is confined within ∼20 degrees of the equatorial plane. The inclination (middle panel) rotates clockwise in a green to yellow colored area that is mostly distributed at the upper part of the current sheet and counterclockwise to a purple to red color portion that is distributed at the lower part of the current sheet. Such rotations are caused mostly by adding an anti-parallel component to the background field lines. It leads to a dipole-like configuration. The clockwise rotation that can be seen at the southern hemisphere leads, however, to a tail-like configuration. Such tendency can be seen at the upper-right corner of the panel.
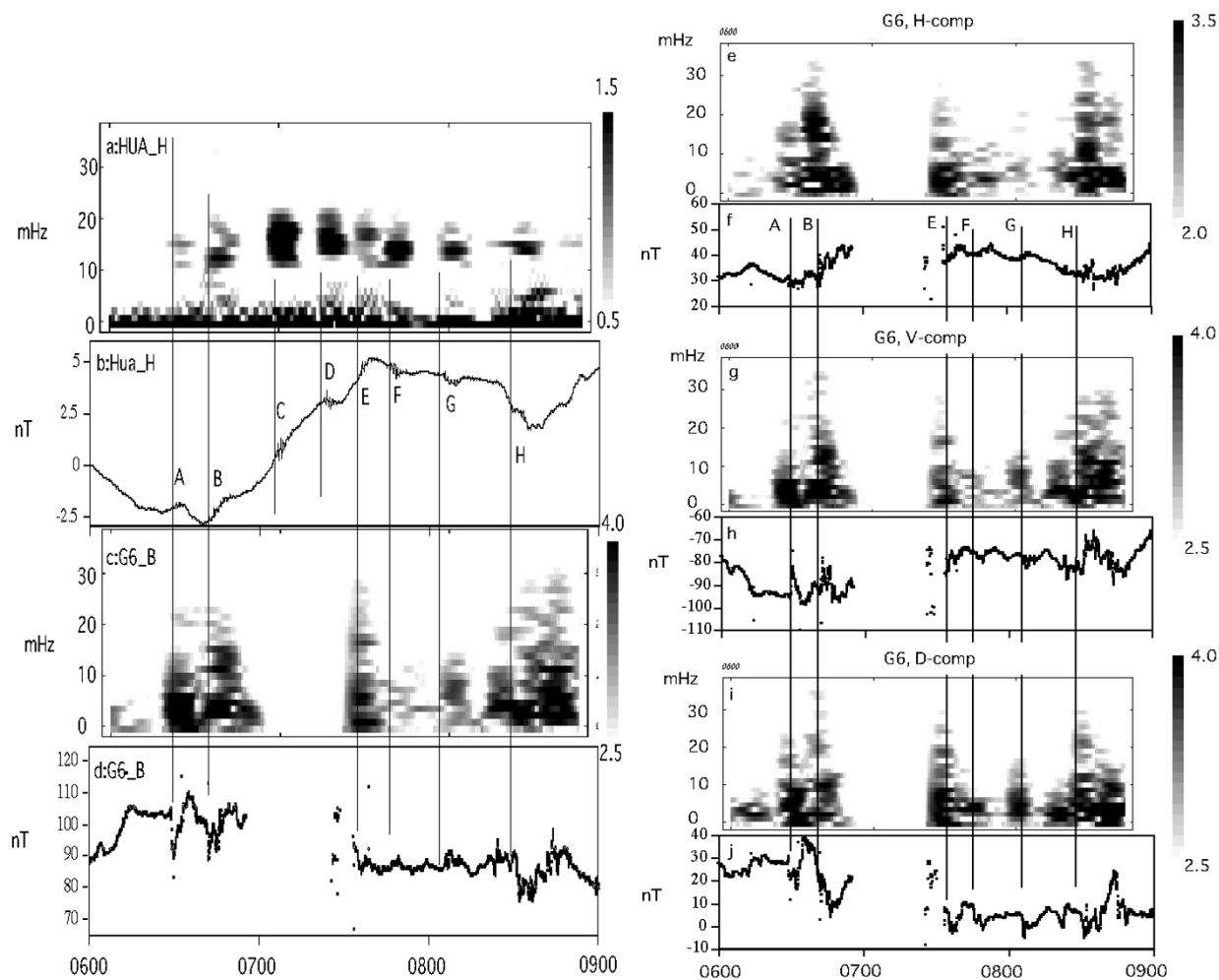
Fig. 4. (a) Dynamic power spectra and (b) plot out of the H component of Huancayo. (c) Power spectra and (d) plot out of field magnitude B of GOES 6 magnetometer data. (e) Dynamic power spectra and (f) plot out of the H component of GOES 6 data. (g) Dynamic power spectra and (h) plot out of the V component of GOES 6 data. (i) Dynamic power spectra and (j) plot out of the D component of GOES 6 data. Power spectra are plotted in logarithmic scale (see right-hand side of the panel). The vertical lines indicate the onset of Pi2.

The dusk-to-dawn currents might be set up at the substorm expansion onset with finite size in LT. At the eastern and western edge of the dusk-to-dawn currents, the currents divert along the field lines to make the current closure (Fujita *et al.*, 2002). For the diamagnetic current case, the diversion would take place from the non-uniform pressure region located in the dawn and dusk sector (Saka *et al.*, 1996). The field-aligned currents reflected from the ionosphere establish the toroidal mode waves in the dawn and dusk sector remote from the midnight sector (Saka *et al.*, 1996; Fujita *et al.*, 2002). As a result, dusk-to-dawn currents connected to the field-aligned currents modulate the current intensity at the oscillation frequency of the toroidal mode. Waveforms of the field magnitudes thus produced by the modulation of the dusk-to-dawn currents are schematically depicted at three different locations in the bottom of the figure. Signal disappears at the demarcation region. The waveform changes oppositely besides the demarcation region.

4. Comparison of GOES 6 Data with the Model

We suggest that the GOES 6 satellite encountered the dusk-to-dawn currents first at the negative B region during

events "A", "B", and "E". Thereafter, the satellite encountered at positive B region ("F" and "G"), followed by an encounter with the negative B region during "H" event. Examination of the V component suggests that during the events "A", "B", and "E", the GOES 6 satellite was located at a position north of the dusk-to-dawn current because the polarity of the V component was positive (radial outward). For "F" and "G", the satellite was to the south of the dusk-to-dawn currents because the V component was negative. Then, the satellite was back to the north of the dusk-to-dawn currents during the "H" event. In the dipole system, the GOES 6 satellite would be located 5 to 11 degrees north of the equatorial plane. To account for the GOES 6 observation of the event "F" and "G", we suggest that the current sheet may be located outside of the equatorial plane. In the dipole field model, however, such a current sheet location is difficult to consider because the plasmas are supposed to be injected along the equator. Therefore, a plausible explanation for these events could be made by plasma instabilities (e.g., Lui *et al.*, 1999) that energize the background plasmas locally in the midnight sector and intensify the plasma pressures thereabouts. The examination of the plasma processes associated
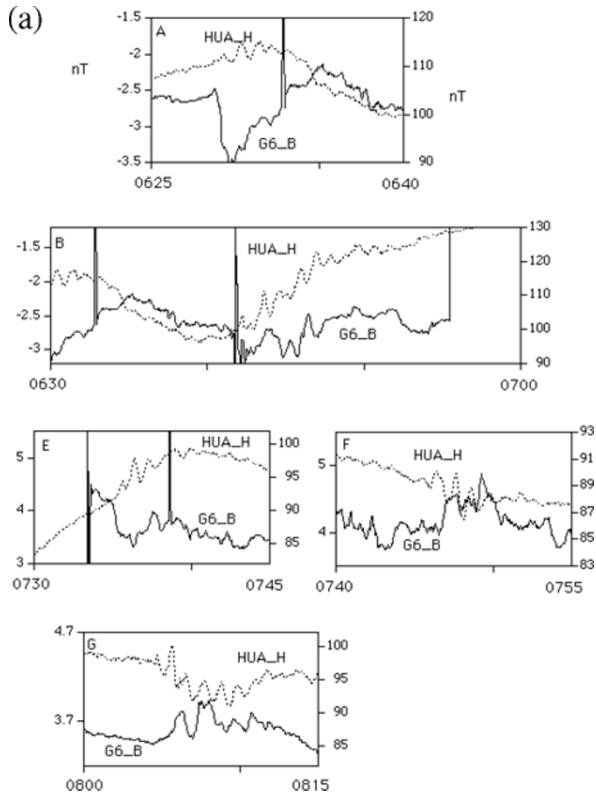
Fig. 5(a). Waveform comparison between the H component of Huancayo (dashed lines) and field magnitude B of GOES 6 altitudes (solid lines) for the event "A" through "G", except for "C" and "D". The event "H" is not shown because of a less clear waveform of the ground data and large background field changes in the satellite data (not in the Pi2 band). Scales (nT) are to the right for the satellite, to the left for the ground. Spikes are noises of the GOES 6 magnetometer.
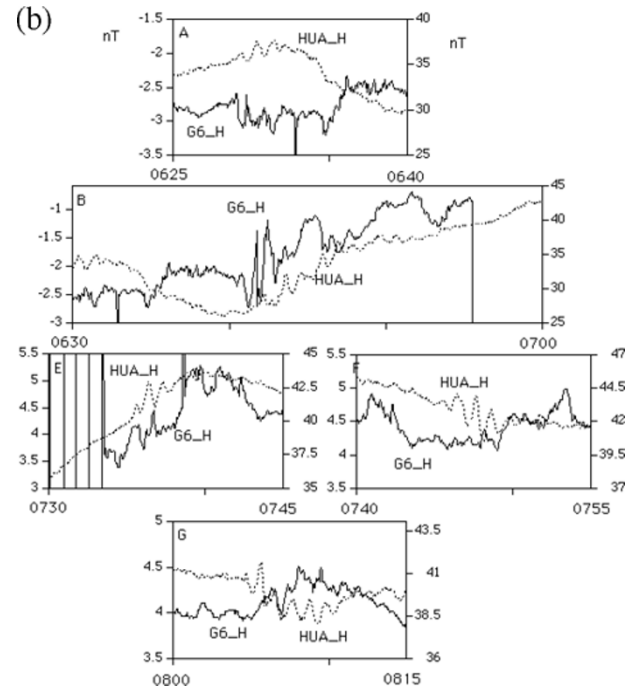

Fig. 5(b). Same as for Fig. 5(a) but for the H component of GOES 6 satellite.
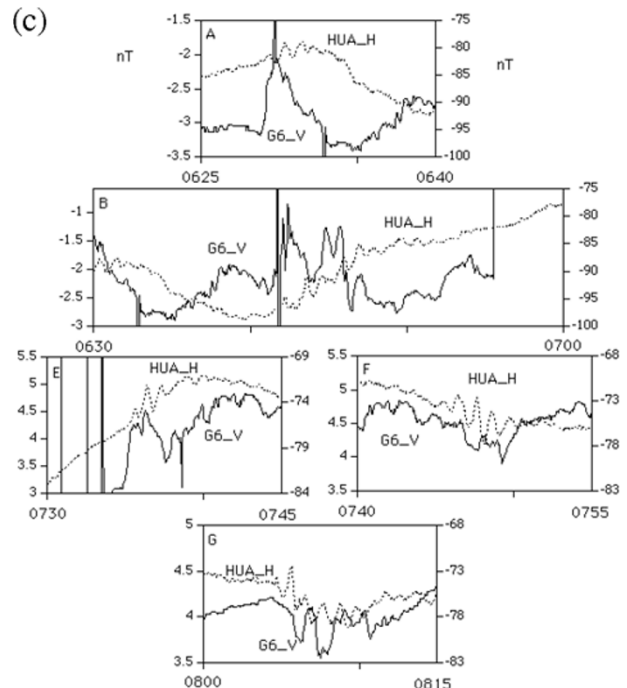
Fig. 5(c). Same as for Fig. 5(a) but for the V component of GOES 6 satellite.

with the formation of current sheet in the midnight magnetosphere might be beyond the scope of the present study.

The field changes at the GOES 6 position during the multiple Pi2 events were estimated to be ∼25 nT for the V component and ∼15 nT for the H component. Therefore, the field magnitude of about 30 nT could be added at $L = 6.6$ to the background fields.

Figure 4 shows dynamic power spectra of the H component calculated from (a) ground station and from (c) the field magnitudes of GOES 6. The original plots at these two locations are also presented in (b) and (d), respectively. Although a gap appears in the GOES data, a good correlation can be seen between the occurrence of the ground Pi2 train and the corresponding disturbances of the field magnitudes at geosynchronous altitudes. Note that the original magnetometer data are band-pass filtered (33–333 mHz) before power spectral analysis. The power spectra were calculated by the FFT technique by use of 256 data points sampled at 3-sec. The spectra of the GOES data are distributed in wider frequency range than those of the ground data. The spectra and original plots of the components H, V, and D of the GOES 6 satellite are presented in the Fig. 4(e) to (j). The D component plot in Fig. 4(j) shows a decrease of amplitude at all the Pi2 onset. This feature is consistent with the occurrence of the downward field-aligned currents in the vicinity of the GOES 6 satellite. The associated fluctuations of the D

component could be attributable to the amplitude oscillation of the downward field-aligned currents of the substorm current wedge system. The power spectra for the components H (Fig. 4(e)), V (Fig. 4(g)), D (Fig. 4(i)) and field magnitudes (Fig. 4(c)) seemed to be composed roughly of the spectral band below and above 10 mHz. Nevertheless, detailed structures of the spectra do not match. There are reasons why the spectral structures do not match. First, the H and
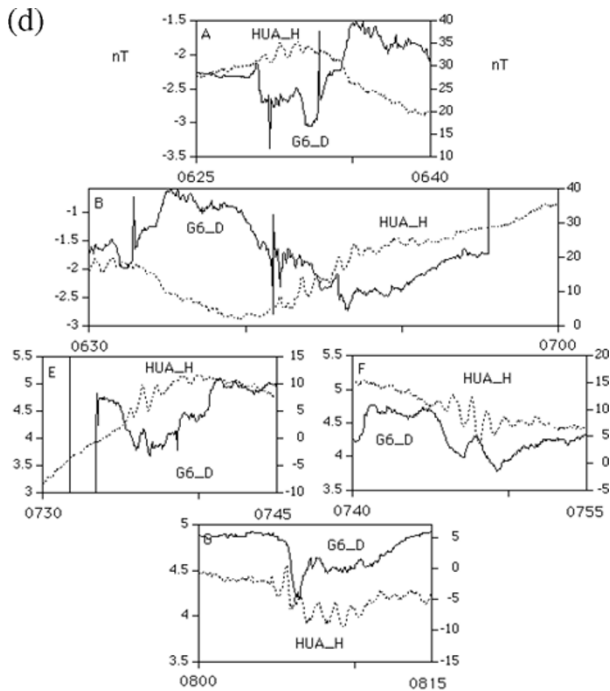
(d)

Fig. 5(d). Same as for Fig. 5(a) but for the D component of GOES 6 satellite.

5. Summary

We examined the GOES 6 magnetometer data in the midnight sector during a Pi2 event. Our findings are summarized as follows;

(1) The field magnitudes and field line inclinations of the GOES 6 magnetometer data can be accounted for by the formation of the dusk-to-dawn currents in the vicinity of the geosynchronous altitudes. (2) The GOES6 satellite was located to the north/south of the dusk-to-dawn currents during the Pi2 event. (3) The intensity of the dusk-to-dawn current shows wide band fluctuations and may launch poloidal mode of waves that contain the Pi2 band oscillations.

It has been suggested by the computer simulation that the dusk-to-dawn current in the midnight sector and field-aligned current diverted from it are source of the Pi2 pulsation in the magnetosphere (Fujita *et al.*, 2000, 2002). The present study provides observational supports for this belief.

References

Akasofu, S.-I., The development of auroral substorm, *Planet. Space Sci.*, **12**, 273–282, 1964.

Baker, D. N. *et al.*, Neutral line model of substorms: Past results and present view, *J. Geophys. Res.*, **101**, 12975–13010, 1996.

Fujita, S., M. Itonaga, and N. Nakata. Relation between the Pi2 pulsations and the localized impulsive current associated with the current disruption in the magnetosphere, *Earth Planets Space,* **52**, 267–281, 2000.

Fujita, S., H. Nakata, M. Itonaga, A. Yoshikawa, and T. Mizuta. A numerical simulation of the Pi2 pulsations associated with the substorm current wedge, *J. Geophys. Res.*, **107**, SMP2-1–2-15, 2002.

Lui, A. T. Y., K. Liou, M. Nose, S. Ohtani, D. Williams, T. Mukai, K. Tsuruda, and S. Kokubun, Near-Earth dipolarization: evidence for a non-MHD process, *Geophys. Res. Lett.*, **26**, 2905–2908, 1999.

Olson, J. V., Pi2 pulsations and substorm onsets: A review, *J. Geophys. Res.*, **104**, 17499–17520, 1999.

Reeves, G. D., T. A. Fritz, T. E. Cayton, and R. D. Belian, Multi-satellite measurements of the substorm injection region, *Geophys. Res. Lett.*, **17**, 2015–2018, 1990.

Saka, O., H. Akaki, O. Watanabe, and D. N. Baker, Ground-satellite correlation of low-latitude Pi2 pulsations: A quasi-periodic field line oscillation in the magnetosphere, *J. Geophys. Res.*, **101**, 15433–15440, 1996.

Saka, O., K. Okada, O. Watanabe, D. N. Baker, G. D. Reeves, and R. D. Belian, Pi2-associated particle flux and magnetic field modulations in geosynchronous altitudes, *J. Geophys. Res.*, **102**, 11363–11373, 1997.

Sakurai, T. and R. L. McPherron, Satellite observations of Pi2 activity at geosynchronous orbit, *J. Geophys. Res.*, **88**, 7015–7027, 1983.

Shiokawa, K., W. Baumjohann, and G. Haerendel, Braking of high-speed flows in the near-Earth tail, *Geophys. Res. Lett.*, **24**, 1179–1182, 1997.

Takahashi, K., S-I. Ohtani, and K. Yumoto, AMPTE CCE observations of Pi2 pulsations in the inner magnetosphere, *Geophys. Res. Lett.*, **19**, 1447–1450, 1992.

Takahashi, K., S-I. Ohtani, and B. J. Anderson, Statistical analysis of Pi2 pulsations observed by the AMPTE CCE spacecraft in the inner magnetosphere, *J. Geophys. Res.*, **100**, 21929–21941, 1995.

Takahashi, K., B. J. Anderson, and S-I. Ohtani, Multisatellite study of nightside transient toroidal waves, *J. Geophys. Res.*, **101**, 24815–24825, 1996.

Yeoman, T. K. *et al.*, A comparison of midlatitude Pi 2 pulsations and geostationary orbit particle injections as substorm indicators, *J. Geophys., Res.*, **99**, 4085–4094, 1994.

Yumoto, K., et al., Some aspects of the relation between Pi1–2 magnetic pulsations observed at $L = 1.3$–2.1 on the ground and substorm-associated magnetic field variations in the near-Earth magnetotail observed by AMPTE CCE, *J. Geophys. Res.*, **94**, 3611–3618, 1989.

O. Saka (e-mail: saka@kurume-nct.ac.jp), H. Akaki, and D. N. Baker

V component represent primarily the oscillation of dusk-to-dawn current that might be connected to both the downward and upward field-aligned currents that close via the ionosphere. Therefore, the oscillations of the H and V component could be affected by the oscillations of field-aligned current pair. While the D component represents primarily the oscillation of the downward component of the field-aligned current. Second, the waveform of H, V and B may change when the current sheet position moved with respect to the satellite location. The recorded waveform however, might not be identical among the components. The waveform comparisons for the events "A" through "G" of B component, H component, V component, and D component are demonstrated in Fig. 5(a), 5(b), 5(c), and 5(d), respectively. It is apparent that the satellite signals are composed of initial increase/decrease of the amplitude and the following oscillating waveforms. Those initial changes and the onset of Pi2's are almost coincident, except for the event "F". This event shows a delay of the field changes at GOES 6 altitudes and contains weak power of the oscillations. We suppose that satellite waveforms are attributable to the impulsive current effect and associated oscillations of the dusk-to-dawn currents and diverted field-aligned currents. The spectral components of the field magnitude B in the GOES 6 magnetometer data are filtered out by the poloidal resonance (plasmasphere virtual resonance and cavity resonance) during transmission across the inner magnetosphere. The poloidal resonance would have smoothed the waveform and changed the spectral components of the satellite signals. It is likely that the spectral power above 10 mHz at the GOES 6 altitudes might appear on the ground station, Huancayo.